══════════ **RADIATION METHODS** ══════════

Estimating the Efficiency of Two Algorithms for Segmentation of Digital Radiation Images of Test Objects

S. E. Vorobeichikov[a], *, V. A. Fokin[b], **, V. A. Udod[a, c], ***, and A. K. Temnik[c], ****

[a]*Tomsk State University, Tomsk, 634050 Russia*
[b]*Siberian State Medical University, Tomsk, 634055 Russia*
[c]*Institute of Nondestructive Testing, Tomsk Polytechnic University, Tomsk, 634050 Russia*
*e-mail: sev@mail.tsu.ru
**e-mail: FokinVasAl@yandex.ru
***e-mail: pr.udod@mail.ru
****e-mail: temnik_ak@mail.ru
Received July 4, 2016

Abstract—A mathematical model that describes digital radiation images of test objects is presented. Two algorithms are given for automatic segmentation of digital images distorted by additive noises. The efficiency of the algorithms is estimated based on mathematical modeling.

INTRODUCTION

The modern level of development of different means and methods of nondestructive testing is characterized by an extensive use of image recognition theory for automatic detection and classification of flaws [1−5]. Along with applications to technical defectoscopy and diagnostics, image recognition algorithms are widely used in inspection systems installed at airports, railway and border crossing stations, state institutions, etc. to ensure transportation safety and prevent smuggling of forbidden items [6].

On the content level, image recognition algorithms are structurally divided into two main (consecutively executed) parts. At the first stage, an image is split into separate segments (image segmentation), followed by recognition of selected segments based on a certain set of signs.

In automatic recognition problems, segmentation is aimed at automatic partitioning of the original image into embedded images of objects that a computer can "see" and recognize based on the thoroughly studied pattern recognition methods [7, 8]. It is evident that image segmentation significantly affects the analysis and recognition of the image as a whole.

Along with "geometrical" recognition, i.e., the recognition of the form (configuration) of defects in a test object (TO) (for example, see [5, 9]), image segmentation is also crucial for "physical" recognition of foreign inclusions in TOs. The latter consists in identifying the material of an inclusion (especially, in customs inspections), for example, by the (effective) atomic number of the inclusion material using dedicated processing of TO radiation images based on the dual energy method [10−12].

Two algorithms for recognizing defect images on radiation patterns of TOs were presented earlier and evaluated in terms of their efficiency (see [5]). In this article, with regard for the own value of image segmentation procedures, we present and evaluate the efficiency of two automatic algorithms for segmentation of digital radiation images of TOs that are constituent elements of the algorithms in [5].

STATEMENT OF THE PROBLEM

A digital image $B(i, j)$ is described, similar to [5], by a relation of the form

$$B(i, j) = B_{\mathrm{b}} + \sum_{m=1}^{M} F_m(i, j) + B_{\mathrm{n}}(i, j). \tag{1}$$

where B_b is the background signal; M is the number of objects in the image;

$$F_m(i, j) = B_m(i, j) - B_b \tag{2}$$

is a function that describes image "brightness" variations (signal component) due to the presence of the m-th object in the image; and

$$B_m(i, j) = \begin{cases} b_m, (i, j) \in Q_m \\ 0, (i, j) \notin Q_m \end{cases} \tag{3}$$

is a function that describes the "brightness" distribution for the m-th object [b_m is the "brightness" of the m-th object in the domain of its localization Q_m; $B_n(i, j)$ is noise due to the quantum nature of radiation; i, j are the integer coordinates of an element (count) of the digital image].

In what follows, it is assumed that:

—the localization domains Q_m ($m = 1, 2, ..., M$) of different objects are pairwise disjoint;

—the separate noise counts $B_n(i, j)$, i.e., noise components that correspond to different pairs (i, j) are independent random variables with the zero mathematical expectation.

Allowing for the above assumptions, the set of relations (1)−(3) can be interpreted as a mathematical model of the digital radiation image of a TO that includes M local inclusions to be revealed.

The aim of this article is to evaluate the efficiency of two automatic algorithms for segmentation of digital radiation images of TOs that are part of the pattern recognition algorithms presented in [5].

In what follows, we describe the above algorithms and the results of mathematical modeling of their efficiencies.

THE FIRST SEGMENTATION ALGORITHM

This algorithm essentially consists in segmenting an image based on its prefiltering with subsequent binarization and includes several main stages [5].

Stage 1. Pre-processing of image $B(i, j)$ that consists in its smoothing for noise level reduction (using the median-smoothing or moving-average methods). A smoothed image $B_s(i, j)$ is formed as a result.

Stage 2. Determining the maximum B_{max} and minimum B_{min} values of the smoothed image $B_s(i, j)$.

Stage 3. Calculating the "brightness" threshold of the smoothed image as

$$p = a \frac{B_{max} + B_{min}}{100\%},$$

where a is the binarization threshold expressed as percentage.

Stage 4. Binarization of the smoothed image that results in a binary image

$$B_b(i, j) = \begin{cases} 1, B_s(i, j) \geq p \\ 0, B_s(i, j) < p \end{cases}.$$

Stage 5. Segmentation of the binary image $B_b(i, j)$, with each segment being the totality of elements (i, j) that form a connected set D and satisfy the condition $B_b(i, j) = 1$.

Stage 6. Discriminating the image segments by area. This operation essentially consists in setting $B_b(i, j) = 0$ for elements with the area of less than S_{thr}, i.e., in "transferring" these elements into the background domain of the binary image.

THE SECOND SEGMENTATION ALGORITHM

The essence of this algorithm is to segment the studied image using the cumulative sum procedure. The algorithm consists of several stages that are listed and described below [5].

Stage 1. Line-by-line segmentation of $B(i, j)$, namely, an image $B(i, j)$ is "viewed" line-by-line and homogeneity (line) segments where the mathematical expectation of counts can be considered constant

are identified in each line. To this end, the cumulative sum (CUSUM) procedure [13−15] designed for detecting the moment when the mathematical expectation starts to increase in the sequence of independent and random variables is used. This procedure is defined by the formulae

$$S_j = \max(S_{j-1} + x_j - \hat{B}_b - \delta, 0), \; S_0 = 0, \; j = 1, \ldots, n,$$

where S_j is the accumulated (cumulative) sum that is used to make a decision that a segment with an increased mathematical expectation has started; x_j is the j-th image count in the current line, i.e., $x_j = B(i, j)$ for a fixed value of i; $\hat{B}_b$ is an estimate of the background B_b over the image $B(i, j)$; δ is a procedure parameter; and n is the length of an image line.

The decision about a change in the mathematical expectation in the observed sequence is made if $S_j > h$, where h is a given positive threshold (an additional procedure parameter). The quantity equal to $j + 1$ is chosen as an estimate for the moment of a mathematical-expectation jump, where j is the last value for which $S_j = 0$.

It should be noted that the CUSUM procedure is directed towards revealing a one-time increase in the mathematical expectation of the observed signal, after which the obtained value j is stored and the process is continued until the current line is over. An array of estimates is thus formed for the left boundaries of the segments where the mathematical expectation is considerably different from $\hat{B}_b$. The estimates for the right segment boundaries are determined similarly when the lines are viewed from right to left.

For the CUSUM procedure to be used practically, it is recommended to select the involved parameters δ and h as follows:

$$\delta = 1/2\Delta,$$

where Δ is the expected value of the minimum jump of mathematical expectation in the image (the minimum value of signal components) due to the presence of flaws in the TO, and

$$1.5\delta \leq h \leq 3\delta.$$

Stage 2. Estimating the average value of counts in each line segment.

Stage 3. Amplitude selection of line segments. A line segment is "transferred" to the background domain if the estimate of the average value of counts on this segment, as calculated at Stage 2, only insignificantly differs from the value $\hat{B}_b$ (for example, by less than $1/3\Delta$). Otherwise, the segment is "kept intact", that is, the estimate of the average value obtained at Stage 2 is retained for this segment.

Stage 4. Formation of image segments, i.e., connected two-dimensional arrays, by combining the line segments along the rows.

Stage 5. Discriminating the image segments by area. Image segments with the area of less than a preset threshold S_{thr} are "transferred" into the image background domain. Unlike in [5], in this case one more operation is performed (one more stage is added). The operation consists in the image $B(i, j)$ being one-dimensionally smoothed "row-wise" by the three-element moving-average method in order to reduce the noise level. This extra operation is performed at the very beginning of the algorithm, prior to Stage 1.

ESTIMATING THE EFFICIENCY OF THE SEGMENTATION ALGORITHMS

The algorithms were tested with images of 300×300 elements, with one object (its digitized version, to be precise)—a square, a circle, or a triangle—of a certain area being generated in each of the images, followed by pollution of the image with an additive noise. The area of an object was understood to be the number of elements (counts) that fell inside or on the border of the analogue object when it was superimposed on a square discretization grid (similar to a checked exercise-book sheet). The background value was taken to be 100, and the difference Δ between the "brightnesses" of the object and the background (signal component, jump in the image mathematical expectation) was equal to 10. Noise counts were assumed to be distributed normally by the same law. The ratio of the signal component (mathematical-expectation jump) to the root-mean-square value of noise (SNR) varied from 1.5 to 3, while the threshold area S_{thr} for discrimination of "small-sized" segments was set at half the area S of the generated object.
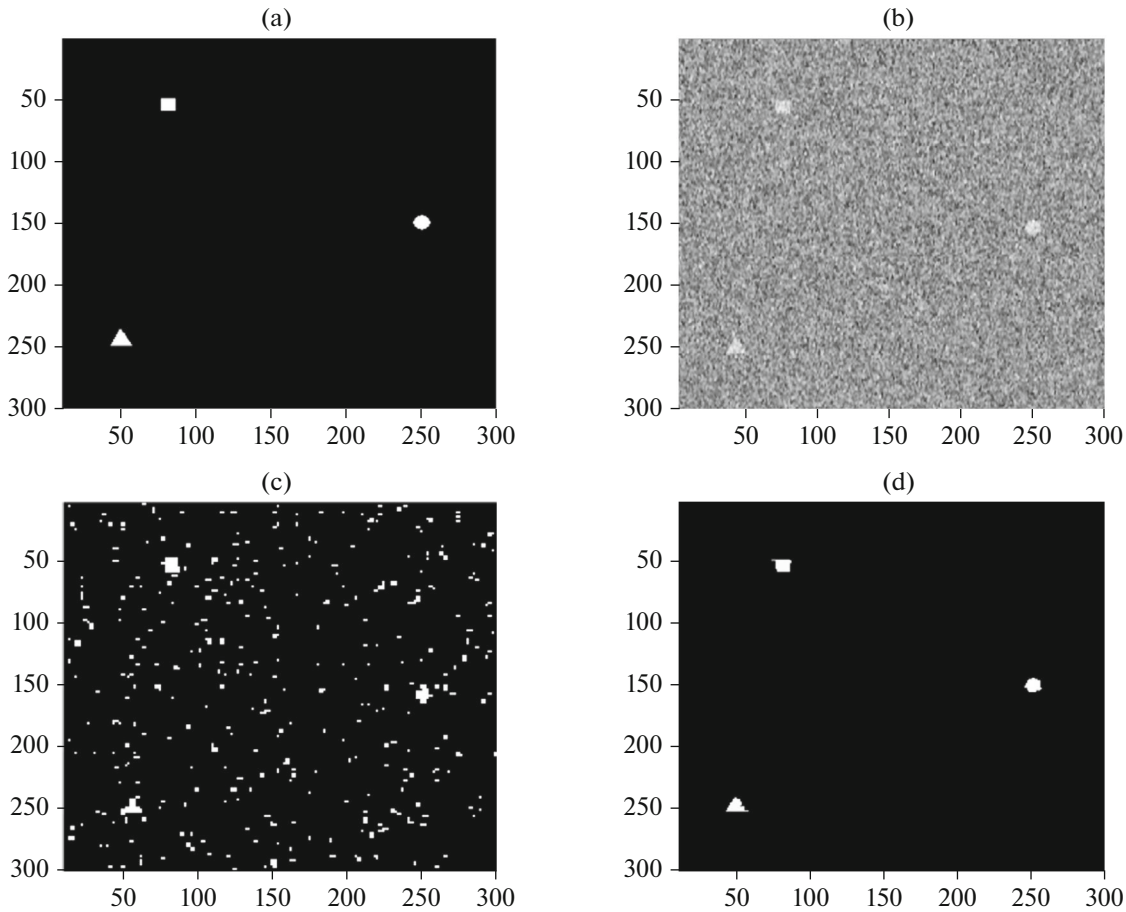
Fig. 1. Example of using segmentation algorithms presented visually as a distorted digital image and the results of its processing: (a) original (ideal) digital image with three "equibright" objects: a square with $S = 100$, a circle with $S = 108$, and a triangle with $S = 104$; (b) the result of distorting the original image by additive noise with an NSR of 1.5; (c) the result of processing the distorted image by the first segmentation algorithm; (d) the result of processing the distorted image by the second segmentation algorithm.

A quantitative estimate of the efficiency of segmentation algorithms was the probability (percentage) of incorrect classification of image elements (the likelihood of erroneous assignment of the image element to the object or the background) [16], that is,

$$p_{\mathrm{err}} = \frac{d_{\mathrm{total}}}{N_{\mathrm{total}}}, \tag{4}$$

where d_{total} is the total number of erroneously classified image elements and N_{total} is the overall dimension (the total number of elements) in the image being segmented.

Apparently, given the value of the parameter N_{total}, the quality of segmentation is unambiguously characterized by the parameter d_{total}.

It can be easily seen that for an image that contains only one object (segment), the quantity d_{total} can be analytically represented as

$$d_{\mathrm{total}} = d + S_{\mathrm{art}}.$$

Here

$$d = \left| (\hat{D} \setminus D) \cup (D \setminus \hat{D}) \right|$$

is the inaccuracy of extracting the original object (segment) D against a noisy background; $\hat{D}$ is the segment extracted by the algorithm (an estimate of the segment D); $(\hat{D} \setminus D) \cup (D \setminus \hat{D})$ is the symmetric differ-
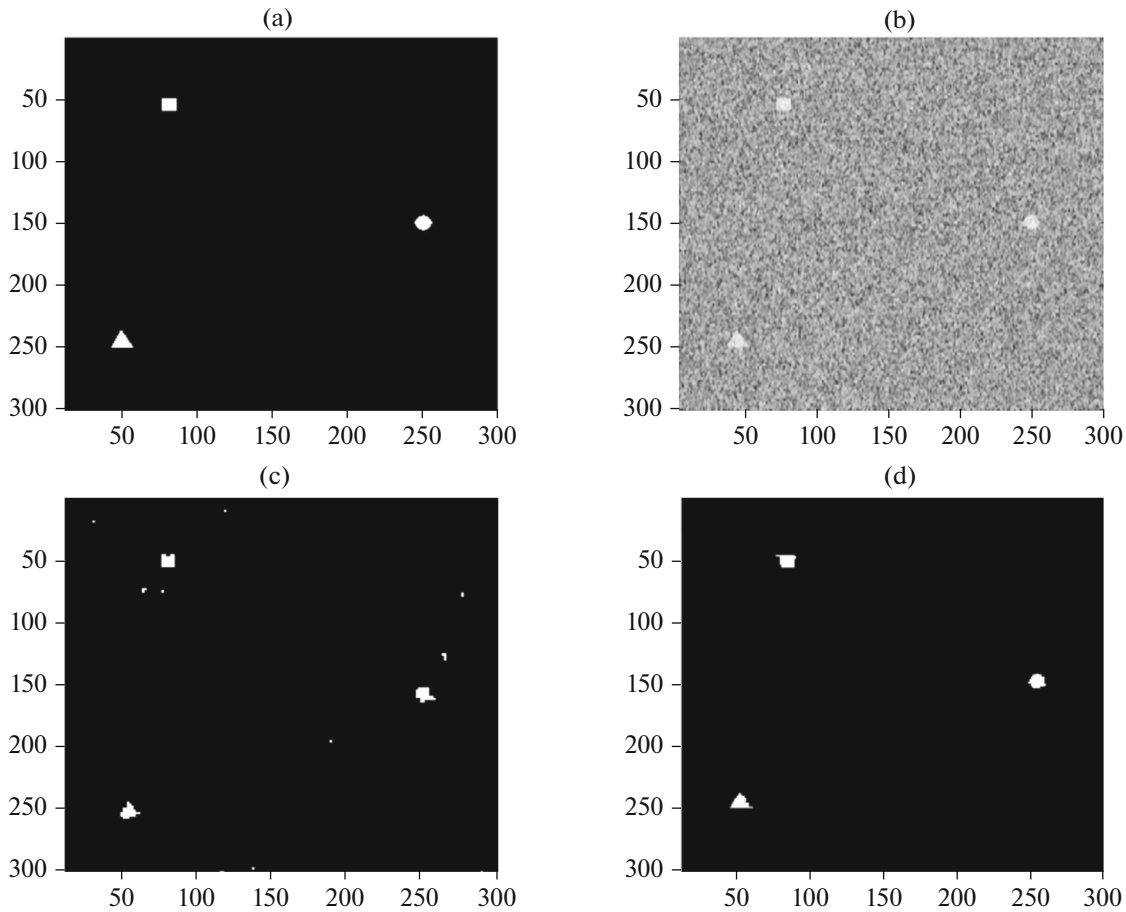
Fig. 2. Example of using segmentation algorithms presented visually as a distorted digital image and the results of its processing: (a) original (ideal) digital image with three "equibright" objects: a square with $S = 100$, a circle with $S = 108$, and a triangle with $S = 104$; (b) the result of distorting the original image by additive noise with an NSR of 2; (c) the result of processing the distorted image by the first segmentation algorithm; (d) the result of processing the distorted image by the second segmentation algorithm.

ence of the sets (segments) D and $\hat{D}$; the vertical lines designate the cardinal number of a set (the number of its elements); and S_{art} is the total area of fake objects (artifacts) that have been extracted by the algorithm in the noisy image. Following [5], the fake object (artifact) is understood to be an object with an area of more than S_{thr} that has been extracted from the noisy background but, in fact, does not exist on the original image (a false alarm).

One hundred images were modeled for each set of parameters of the object and background. Each of the generated 100 images was subjected to segmentation with the above two algorithms, with the first algorithm being used under the following conditions:

—image smoothing with a 3×3 window;

—a binarization threshold of 50% (it is approximately the value that was obtained at the stage of preliminary mathematical modeling of image segmentation for different object areas and SNR values).

In the second algorithm, a threshold of $h = 2\delta = \Delta = 10$ was used for the cumulative sum.

The results of modeling the efficiency of the algorithms are presented in Figs. 1 and 2 and Tables 1–6. The total number of erroneously classified image elements (the parameter d_{total}) was calculated by averaging over 100 image instances.

It can be seen from the data in the figures and the tables that the second segmentation algorithm significantly excels the first one in terms of accuracy. Therefore, it is reasonable to take the second algorithm as a basis for referencing other algorithms with the same function and for its further adaptation to the seg-

Table 1. Total number of erroneously classified image elements (parameter d_{total}) for an original object (segment) in the form of a square versus the object area (the number of elements) and the SNR value for the first segmentation algorithm

S	SNR			
	1.5	2	2.5	3
16	>10000	8523	1384	83
25	>10000	5480	379	8
36	>10000	3116	89	8
49	>10000	2216	39	8
64	>10000	1931	27	9
81	>10000	1419	21	8
100	>10000	1005	20	9

Table 2. Total number of erroneously classified image elements (parameter d_{total}) for an original object (segment) in the form of a circle versus the object area (the number of elements) and the SNR value for the first segmentation algorithm

S	SNR			
	1.5	2	2.5	3
12	>10000	>10000	3223	316
24	>10000	5973	978	43
48	>10000	2370	47	9
75	>10000	1834	22	9
108	>10000	892	20	10

Table 3. Total number of erroneously classified image elements (parameter d_{total}) for an original object (segment) in the form of a triangle versus the object area (the number of elements) and the SNR value for the first segmentation algorithm

S	SNR			
	1.5	2	2.5	3
13	>10000	>10000	4206	418
25	>10000	6676	960	11
46	>10000	2941	78	12
72	>10000	1653	30	13
105	>10000	1291	29	14

Table 4. Total number of erroneously classified image elements (parameter d_{total}) for an original object (segment) in the form of a square versus the object area (the number of elements) and the SNR value for the second segmentation algorithm

S	SNR			
	1.5	2	2.5	3
16	8.47	5.45	4.50	3.90
25	9.31	4.74	3.99	3.68
36	7.82	3.98	2.72	2.00
49	8.89	4.49	2.16	1.30
64	9.44	4.52	2.13	1.16
81	10.44	4.34	2.23	1.07
100	10.18	4.48	2.07	1.11

Table 5. Total number of erroneously classified image elements (parameter d_{total}) for an original object (segment) in the form of a circle versus the object area (the number of elements) and the SNR value for the second segmentation algorithm

S	SNR			
	1.5	2	2.5	3
12	37.29	7.24	6.05	6.95
24	31.75	7.48	6.20	5.39
48	34.67	7.71	6.42	5.65
75	37.15	9.55	7.13	6.30
108	37.45	9.98	8.05	6.83

Table 6. Total number of erroneously classified image elements (parameter d_{total}) for an original object (segment) in the form of a triangle versus the object area (the number of elements) and the SNR value for the second segmentation algorithm

S	SNR			
	1.5	2	2.5	3
13	32.47	8.94	8.55	8.93
25	25.98	7.75	7.12	6.20
46	30.98	8.93	6.86	5.95
72	38.63	10.61	8.08	6.48
105	35.89	11.75	8.92	7.07

mentation of actual digital radiation images of tested objects, in particular, those generated by X-ray inspection systems with the dual energy method [17].

REFERENCES

1. Vavilov, V.P., *Infrakrasnaya termografiya i teplovoi kontrol"* (Infrared Thermography and Thermal Testing), Moscow: Spektr, 2013.
2. Barkhatov, V.A., Recognizing imperfections with an artificial neural network of a special type, *Russ. J. Nondestr. Testing*, 2006, vol. 42, no. 2, pp. 92−100.
3. Syryamkin, V.I. and Gorbachev, S.V., Applying neural network algorithms for the analysis of images of materials in X-ray microtomograms, *Izv. Vyssh. Uchebn. Zaved., Fiz.,* 2013, vol. 56, no. 10/2, pp. 29−34.
4. Grigorchenko, S.A. and Kapustin, V.I., Recognizing imperfections with an artificial neural network of a special type, *Russ. J. Nondestr. Testing*, 2009, vol. 45, no. 9, pp. 648−659.
5. Vorobeichikov, S.E., Fokin, V.A., Udod, V.A., and Temnik, A.K., A study of two image-recognition algorithms for the classification of flaws in a test object according to its digital image, *Russ. J. Nondestr. Testing*, 2015, vol. 51, no. 10, pp. 644−651.
6. Han, Y.-P., Han, Y., Wang, L.-M., and Pan, J.-X., Development of X-ray digital radiography automatic inspection system for testing the interior structure of complex product, *Binggong Xuebao/Acta Armamentarii,* 2012, vol. 33, no. 7, pp. 881−885.
7. Tou, J.T. and Gonsalez, R.C., *Pattern Recognition Principles*, Reading, Massachusetts: Addison-Wesley Publishing Company, 1974.

8. Zhuravlev, Yu.I., *Ob algebraicheskom podkhode k resheniyu zadach raspoznavaniya ili klassifikatsii. Problemy kibernetiki* (On an Algebraic Approach to Solving Recognition or Classification Problems. Problems of Cybernetics), Moscow: Nauka, 1978.

9. Gurvich, A.K. and Vasil'ev, V.A., Estimating the configuration of flaws in metal production with plane-parallel surfaces by a truncated delta-method, *Kontrol'. Diagn.,* 2013, no. 10, pp. 68−70.

10. Ogorodnikov, S.A., Identifying materials in linac-based radiation customs inspection, *Cand. Sci. (Eng.) Dissertation,* St. Petersburg, 2002.

11. Park, J.S. and Kim, J.K., Calculation of effective atomic number and normal density using a source weighting method in a dual energy x-ray inspection system, *J. Korean Phys. Soc.*, 2011, vol. 59, no. 4, pp. 2709−2713.

12. Gil, Y., Oh, Y., Cho, M., and Namkung, W., Radiography simulation on single-shot dual spectrum X-ray for cargo inspection system, *Appl. Radiat. Isot.*, 2011, vol. 69, no. 2, pp. 389−393.

13. Lorden, G., Procedures for reacting to a change in distribution, *Annals. Math. Statist*, 1971, no. 42, pp. 1897−1908.

14. Pollak, M., Optimal detection of a change in distribution, *Ann. Statist*, 1985, no. 13, pp. 206−227.

15. Vorobeichikov, S.E., On detection of changes in the average value in a sequence of random numbers, *Avtom. Telemekh.*, 1998, no. 3, pp. 50−58.

16. Yanshin, V.V., *Analiz i obrabotka izobrazhenii: printsipy i algoritmy* (Analysis and Processing of Images: Principles and Algorithms), Moscow: Mashinostroenie, 1994.

17. Osipov, S.P., Libin, E.E., Chakhlov, S.V., Osipov, O.S., and Shtein, A.M., Parameter identification method for dual-energy X-ray imaging, *NDT & E Int.*, 2015, vol. 76, pp. 38−42.

Translated by V. Potapchouck